



Simulation experimental investigation of plasma off-normal events on advanced silicon doped CFC-NS31

J.P. Bonal ^{a,*}, C.H. Wu ^b, D. Gosset ^a

^a *Laboratoire de Microscopie et d'Etudes de l'Endommagement, Centre d'Etudes de Saclay, F-91191 Gif-sur-Yvette cedex, France*

^b *EFDA, Max-Planck-Institut für Plasmaphysik, 85748 Garching bei München, Germany*

Abstract

Fusion devices high heat loading due to off-normal events (e.g., plasma disruption, slow transients and ELMs, which can occur during a transition from detached to attached divertor operation) requires high thermal conductivity materials. Therefore, carbon fiber composites (CFCs) with high thermal conductivity are favorable. In the framework of the European Fusion Technology program, a great effort has been made to develop Si doped CFCs. NS31 is a 3D CFC containing about 8–10 at.% of silicon. The previous results showed, that NS31 poses lower chemical erosion, lower tritium retention and higher resistivity to water/oxygen reaction in comparing with undoped CFCs. Off-normal simulation experiments were performed under two conditions: (a) 700 MW/m², 10 ms and (b) slow transient 20 MW/m², 2 and 4 s. NS31 behaved very stable even under these extremely severe conditions. In this paper, the detailed results of simulation experiment on high heat loading due to off-normal events are presented and consequences are discussed.

© 2002 Elsevier Science B.V. All rights reserved.

1. Introduction

The use of carbon fiber composites (CFCs) as limiter, baffle, or divertor plate protection materials in next fusion devices, such ITER-FEAT is attractive due to its low-Z, high thermal shock resistance, good mechanical properties at high temperature and low neutron absorption cross-section. However, CFCs have shown the following limitations: high specific area implying a high tritium inventory; high affinity for hydrogen inducing a high chemical sputtering by formation of hydro-carbon species; an enhanced radiation sublimation at elevated temperature ($T > 1200$ K) and a high rate of reaction with water and oxygen at elevated temperature. It has been observed that adding small concentrations of silicon in CFCs can increase the oxidation resistance in steam, decreases the total tritium retention and reduces the hydro-carbon formation by ions and atomic hydrogen [1]. In addition high heat loading due to off-

normal events such as plasma disruptions or slow transients during 'start-up' operation, requires high thermal conductivity carbon based materials.

In the framework of the European Fusion Technology program, a high thermal conductivity Si doped 3D CFC (NS31) has been developed. This work presents the NS31 thermal properties before and after off-normal simulation experiments.

2. Experimental

2.1. Material

NS31 is a 3D CFC constituted by a NOVOLTEX preform with P55 ex-pitch fibers in the y -direction and ex-PAN fibers in the x -direction; this CFC undergoes a subsequent needling which gives an orientation in the z -direction. The volumetric fraction of fibers is 35% (27% in the y -direction, 4% in both x and z directions). The high thermal conductivity direction is that of P55 ex-pitch fibers (y -direction). The densification is performed by chemical infiltration of pyrocarbon at 1000 °C

* Corresponding author. Tel.: +33-1 6908 5058; fax: +33-1 6908 9082.

E-mail address: jean-pierre.bonal@cea.fr (J.P. Bonal).

followed by a graphitization heat treatment at high temperature. The last phase of densification is made by chemical infiltration of pyrocarbon at 1000 °C followed by a final infiltration of liquid silicon leading partly to the formation of silicon carbide. NS31 contains about 8–10 at.% of silicon, its porosity is about 3–5% and its density is about 2.1 g/cm³.

2.2. Thermal shock tests conditions

In order to test thermal property changes after severe thermal loading, six NS31 samples in the high conductivity direction (y1–y6) have been tested using the European Electron Beam Facility FE 200, located at Le Creusot and managed by Framatome [2].

The mock-up is constituted of a cooled stainless steel plate with six CFC sample holders. Papyex is used in order to insure a uniform thermal contact between the different parts.

The maximum power of the electron beam is 200 kW/cm², but it works in the range 100–120 kW/cm². The electron beam spot diameter is 1.5–2 mm and the sweeping angle is $\pm 10^\circ$ at 10 kHz, so the time for one period of sweeping is 0.1 ms. The surface temperature is measured by two infrared pyrometers, one from 400 to 800 °C and the other from 600 to 2800 °C. For the disruption simulation tests, a fast pyrometer with a temperature ranging from 500 to 2900 °C and an acquisition frequency of 2 kHz has been used.

Two kinds of thermal shock tests have been carried out: 10 ms thermal shock tests at 700 MW/m² (samples y1 and y2), and slow transient tests at 20 MW/m² during 2 and 4 s (samples y3–y6). The thermal shock tests conditions are given in Table 1.

The 10 ms thermal shock tests lead to surface temperature as high as 2900 °C (Table 2). It can be noticed that the initial temperature has to be below 700 °C before each new pulse, for all the samples undergoing several pulses. Moreover, the very high temperatures measured by the infrared pyrometers are difficult to analyse due to the darkening of the windows, especially for the samples y1, y2, y5 and y6. The vacuum during the thermal shock tests is about 10⁻⁴ mbar. At 2200 °C, the total vapor pressure over solid graphite is 10⁻⁴ mbar

Table 1
Thermal shock tests condition

Sample	Pulse duration (ms)	Energy (MJ/m ²)	Power flux (MW/m ²)	Number of pulses
y1	10	7	700	1
y2	10	7	700	5
y3	2000	40	20	22
y4	2000	40	20	10
y5	4000	80	20	10
y6	4000	80	20	20

Table 2
Maximum surface temperatures during 10 ms thermal shock tests

Sample	Serial number of the pulse	Pulse duration (ms)	Maximum surface temperature (°C)
y1	1	10	2844
y2	1	10	2863
	2	10	2887
	3	10	2896
	4	10	2916
	5	10	2922

Table 3
Maximum surface temperatures of y4 sample during 2 s slow transient test

Serial number of the pulse	Pulse duration (s)	Dwell time between two pulses (s)	Maximum surface temperature (°C)	Time to go from T_{\max} to 700 °C (s)
1	2		2167	6.38
2	2	59.45	2275	7.22
3	2	57.18	2334	8.18
4	2	59.45	2363	8.93
5	2	57.18	2385	9.60
6	2	59.45	2401	10.05
7	2	57.17	2508	11.18
8	2	59.46	2547	11.55
9	2	57.17	2549	12.08
10	2	59.46	2586	12.45

[3]. So it is obvious that beyond 2200 °C at 10⁻⁴ mbar, there is a sublimation of carbon leading to a weight loss of the samples.

The 2 s slow transient tests lead to surface temperature of about 2500 °C (Table 3). The 4 s slow transient

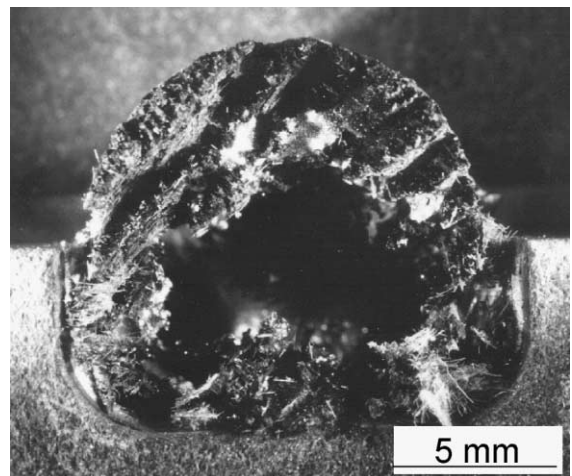


Fig. 1. NS31 3D CFC after 20 pulses of 4 s slow transient test at 20 MW/m².

Table 4
Maximum surface temperatures of y5 sample during 4 s slow transient test

Serial number of the pulse	Pulse duration (s)	Dwell time between 2 pulses (s)	Maximum surface temperature (°C)	Time to go from T_{\max} to 700 °C (s)
1	4		2751	8.25
2	4	116.37	2774	9.53
3	4	116.20	2788	10.05
4	4	116.30	2778	10.50
5	4	116.20	2767	10.43
6	4	116.30	2749	11.03
7	4	116.20	2749	9.90
8	4	116.30	2715	10.20
9	4	116.20	2692	10.43
10	4	116.30	2667	10.13

tests lead to very high surface temperature of about 2800 °C. The y6 sample which has undergone 20 pulses is completely destroyed at the end of the test (Fig. 1). The y5 sample which has undergone 10 pulses (Table 4), shows a large reduction in thickness.

3. Results

3.1. NS31 properties before thermal shock tests

Twelve disks ($\phi = 12$ mm, $h = 5$ mm) have been used for thermal diffusivity measurements before thermal shock tests. Six of them (y1–y6) are in the high thermal conductivity direction (P55 ex-pitch fibers direction); three of them (x1, x2, x3) are in the x -direction (ex-PAN fibers direction) perpendicular to the y -direction; and three of them (z1, z2, z3) are in the needling direction, perpendicular to the xy plane. Six cylinders ($\phi = 4.5$ mm, $h = 7$ mm) have been used for specific heat capacity measurements, and three cylinders ($\phi = 5$ mm, $h = 15$ mm) have been used for thermal expansion measurements.

3.1.1. Density

The samples densities range between 1.94 and 2.13 g/cm³ (Table 5), and the average value is 2.06 g/cm³; value which is in good agreement with the Société Européenne de Propulsion (SEP) value (2.10 g/cm³).

3.1.2. Specific heat capacity

The specific heat capacities of the six samples (two samples in each direction) have been measured with a differential scanning calorimeter Setaram DSC 111G. The NS31 specific heat capacity average values are given in Table 6. At room temperature, the NS31 specific heat capacity is in good agreement with that of NS11, a Si doped CFC, which contains the same amount of silicon

Table 5
NS31 samples densities

Sample	Density (g/cm ³)
y1	2.116
y2	1.942
y3	2.092
y4	1.981
y5	2.132
y6	2.019
x1	2.101
x2	2.082
x3	2.062
z1	2.056
z2	2.084
z3	2.037
Average	2.059

Table 6
NS31 specific heat capacity

Measurement temperature (°C)	Specific heat capacity (J kg ⁻¹ K ⁻¹)
25	690
100	916
200	1127
300	1274
400	1383
500	1466
600	1532
700	1585
800	1629

[4]. Nevertheless NS31 specific heat capacity at 800 °C (1629 J kg⁻¹ K⁻¹) seems to be lower, compared to the NS11 one (1670 J kg⁻¹ K⁻¹).

3.1.3. Thermal diffusivity and thermal conductivity

Thermal diffusivities have been measured by the laser flash method using an apparatus called 'Flash 1000-2'. The thermal diffusivity (D) of the sample is obtained with Parker's method. The samples are disks (diameter: 12 mm; thickness: 5 mm). The method consists in illuminating the front face of these disks with a short heat pulse. The thermal diffusivity is deduced from the heat equation applied to the thermal transient of the rear face, called thermogram. The analysis of the thermograms according to Parker's method allows to solve the heat equation in one dimension; and in the total absence of heat exchange between the sample and the furnace atmosphere, the following equation can be used:

$$D = \frac{\gamma L^2}{t_{1/2}}, \quad (1)$$

where L is the thickness of the sample, $t_{1/2}$ is the time needed to reach 50% of the maximum temperature

increase (T_{max}), and γ is 0.13878. In case that there are heat losses by the front and rear faces of the disk, γ is estimated by a method proceeding from Cowan [5].

The evaluation of the thermal conductivity (K) of each of the 12 NS31 samples is performed using the following equation:

$$K = D\rho C_p, \tag{2}$$

where D is the thermal diffusivity of the sample, C_p is the NS31 average specific heat capacity and ρ is the measured density of the sample. The evaluation of ρ versus temperature is performed using the average linear thermal expansion coefficients (20–800 °C) and is given by the following equation:

$$\rho(T^{\circ}\text{C}) = \frac{\rho(25^{\circ}\text{C})}{1 + [(\alpha_{(x)} + \alpha_{(y)} + \alpha_{(z)}) \times (T^{\circ}\text{C} - 25^{\circ}\text{C})]}, \tag{3}$$

where $\alpha_{(x)}$, $\alpha_{(y)}$ and $\alpha_{(z)}$ are the average linear thermal expansion coefficients (20–800 °C) in x , y and z directions, respectively.

The NS31 average thermal conductivities in the three directions according to Eq. (2) are given in Table 7. The comparison with the SEP thermal conductivity values is in good agreement especially at 800 °C (Table 8).

3.1.4. Thermal expansion

The NS31 average thermal expansion coefficients have been measured in the three directions up to 1000 °C, using dilatometer Setaram DHT 2400 (Table 9).

3.2. NS31 properties after thermal shock tests

3.2.1. Mass and density changes

The y1 and y2 samples which have undergone 10 ms thermal shock tests, show no dimensional changes, but they lost a little of weight, inducing a decrease of their densities (Table 10). Even though the surface temperatures of these samples are 2900 °C, their visual aspects are the same after disruption simulation tests (Fig. 2).

Table 7
NS31 thermal conductivities in the three directions

Temperature (°C)	K_y ($\text{W m}^{-1} \text{K}^{-1}$) ex-pitch fibers direction	K_x ($\text{W m}^{-1} \text{K}^{-1}$) ex-PAN fibers direction	K_z ($\text{W m}^{-1} \text{K}^{-1}$) needling di- rection
25	288	113	104
100	279	114	99
200	250	105	87
300	222	94	76
400	199	83	68
500	180	74	61
600	165	65	56
700	152	58	51
800	142	52	48

Table 8
Comparison of SEP and CEA thermal conductivity values

K ($\text{W m}^{-1} \text{K}^{-1}$)	CEA values	SEP values
K_y at 25 °C	288	304
K_x at 25 °C	113	100
K_z at 25 °C	104	91
K_y at 800 °C	141	149
K_x at 800 °C	52	55
K_z at 800 °C	48	48

Table 9
NS31 average thermal expansion coefficients in the three directions

T (°C)	$\alpha_{(y)}$ (20– T °C) (10^{-6}K^{-1})	$\alpha_{(x)}$ (20– T °C) (10^{-6}K^{-1})	$\alpha_{(z)}$ (20– T °C) (10^{-6}K^{-1})
200	−0.75	0.91	1.46
400	−0.26	1.40	1.95
600	0.12	1.80	2.33
800	0.39	2.12	2.64
1000	0.55	2.35	2.85

Table 10
NS31 dimensional, mass and density changes after thermal shock tests

Sample	Diameter change (%)	Thickness change (%)	Mass change (%)	Density change (%)
y1	0.13	0.22	−1.01	−1.49
y2	0.10	−0.04	−2.34	−2.50
y3	0.33	2.24	−3.93	−6.83
y4	0.33	0.50	−2.32	−3.48
y5	−0.40	Up to 61	−41.31	−

The y3 (22 pulses) and y4 (10 pulses) samples which have undergone 2 s slow transient tests, show a loss of weight of 3.9% and 2.3%. These samples exhibit no change in their visual aspects.

The y6 sample which has undergone 20 pulses of 4 s slow transient test is completely destroyed (Fig. 1). A big hole at the center of the sample has been eroded by the electron beam.

The y5 sample which has undergone 10 pulses of 4 s slow transient test, shows a severe erosion. It has lost 41% of its weight and presents a large reduction in thickness (maximum: 3.1 mm at the center of the disk). A scanning electron microscopy examination shows that matrix (pyrocarbon and silicon) and ex-PAN fibers in the x -direction, have been more easily eroded than P55 ex-pitch fibers bundle in the y -direction (Fig. 3).

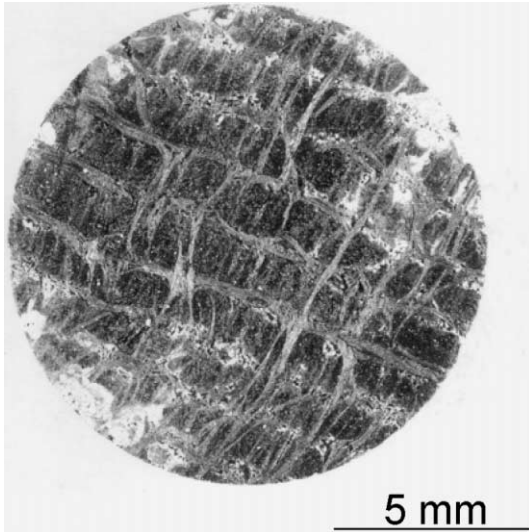


Fig. 2. NS31 3D CFC after five pulses of 10 ms disruption test at 700 MW/m².

3.3. Thermal properties changes

Thermal diffusivities after thermal shock tests have been measured in the same way as before. The y5 sample has been machined so that its surface became flat, therefore its thickness becomes 1.943 mm, and its density 1.713 g/cm³.

The evaluation of the thermal conductivity after thermal shock tests (K_s) is performed according to Eq. (2) with the thermal diffusivity and the density of the sample after thermal shock. The specific heat capacity was assumed to be the same before and after thermal shock. The evaluation of ρ_s versus temperature is performed using Eq. (3). Thermal expansion coefficients are assumed to be the same before and after thermal shocks tests. The thermal conductivity changes are given in the Table 11.

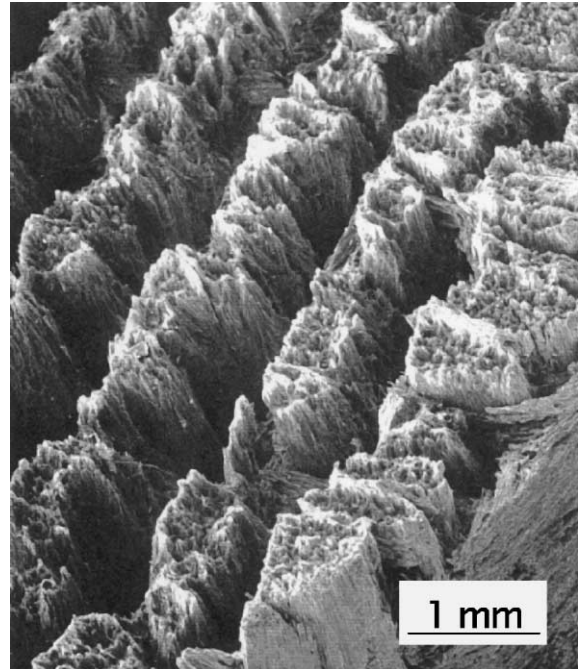


Fig. 3. NS31 3D CFC after 10 pulses of 4 s slow transient test at 20 MW/m².

The samples, which have undergone 10 ms thermal shock tests do not show any change in thermal conductivity, however the y2 sample presents a little increase in thermal conductivity (12–13%) at low measurement temperatures (25/100 °C).

The y4 sample which has undergone 10 pulses of 2 s slow transient test shows also no change in thermal conductivity. But the y3 sample which has undergone 22 pulses of the same slow transient test shows a thermal conductivity decrease of 10/13% from room temperature to 800 °C (Fig. 4).

The y5 sample which has received 10 pulses of 4 s slow transient test, presents a thermal conductivity loss of 25% at 200 °C and 12% at 800 °C (Fig. 5).

Table 11
NS31 thermal conductivity changes after thermal shock tests

Measurement temperature (°C)	Thermal conductivity change ($K_s - K$)/ K (%)				
	y1 sample	y2 sample	y3 sample	y4 sample	y5 sample
25	-4.9	13.0	-12.7	-2.5	
100	-4.4	12.2	-11.3	2.7	
200	-3.8	10.5	-10.4	6.2	-25.4
300	-3.5	7.3	-9.6	7.1	-24.1
400	-2.6	4.9	-9.8	5.7	-22.6
500	-2.4	1.8	-9.9	3.7	-20.0
600	-1.6	-1.3	-10.3	0.0	-17.9
700	-1.2	-3.4	-11.2	-3.6	-15.2
800	0.0	-6.6	-12.2	-7.6	-12.3

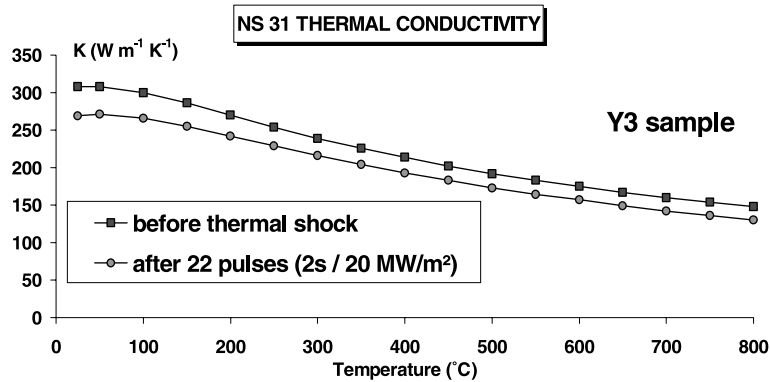


Fig. 4. NS31 thermal conductivity before and after 2 s slow transient test.

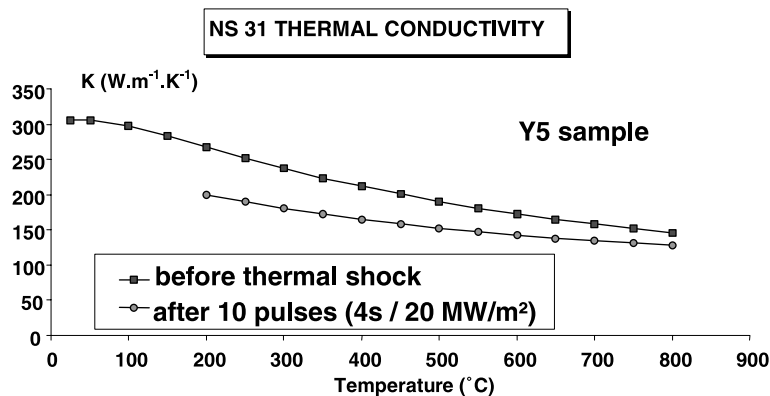


Fig. 5. NS31 thermal conductivity before and after 4 s slow transient test.

4. Conclusion

The main conclusions which can be drawn from the thermal shock tests are the followings:

- For the NS31 samples which have undergone a few pulses of 10 ms thermal shock tests (700 MW/m^2), the surface temperatures reach $2900 \text{ }^\circ\text{C}$. However the samples keep their integrity, and their thermal conductivities do not change.
- The NS31 samples which have undergone 10 or 20 pulses of 2s slow transient tests (20 MW/m^2) have lost a few percent of their weight; and the 20 pulses sample has lost about 10% of its thermal conductivity.
- Twenty pulses of 4 s slow transient test (20 MW/m^2), lead to the destruction of the sample. Ten pulses lead to surface temperatures as high as $2800 \text{ }^\circ\text{C}$, a weight loss of 41% and a thermal conductivity loss which ranges between 25% and 12% in the temperature range $200\text{--}800 \text{ }^\circ\text{C}$.
- Even though very high surface temperatures have been reached during the thermal shock tests, NS31

keeps a good thermal conductivity as long as the erosion is not too high.

Acknowledgements

The authors would like to thank M. Febvre and M. Diotalevi for their valuable help during thermal shock experiments.

References

- C.H. Wu, C. Alessandrini, J.P. Bonal, A. Caso, H. Grote, R. Moormann, A. Perujo, M. Balden, H. Werle, G. Vieider, Fusion Technology 1996, Proceedings of the 19th Symposium on Fusion Technology, vol. 1, p. 327.
- M. Diotalevi, European Electron Beam Facility FE 200 for thermal-hydraulic and thermomechanical testing, thermal tests on NS31 samples (CEA54), final report, Framatome centre technique, Report MC/Ts – MDI/96.498, 1996.
- Groupe Français d'Etude des Carbones, Les Carbones, Masson, Paris, 1965.
- J.P. Bonal, C.H. Wu, J. Nucl. Mater. 277 (2000) 351.
- R.D. Cowan, J. Appl. Phys. 34 (4) (1965) 92.